

IN SITU SOIL PIPEFLOW EXPERIMENTS ON CONTRASTING STREAMBANK SOILS

T. L. Midgley, G. A. Fox, G. V. Wilson, R. M. Felice, D. M. Heeren



ABSTRACT. Soil piping has been attributed as a potential mechanism of instability of embankments and streambanks. Limited field work has been conducted on quantifying and modeling pipeflow and internal erosion processes in the field with either natural or artificially created soil pipes. This research utilized an innovative constant-head trench system to conduct constant-head soil pipe experiments in two contrasting streambanks: Dry Creek in northern Mississippi and Cow Creek in northern Oklahoma. Experiments included open pipes, in which the soil pipe was directly connected to the constant-head trench and open at the streambank face, and clogged pipes, which involved plugging the outlet of the soil pipe using soil excavated adjacent to the pipe. A tensiometer network was used to measure soil water pressures surrounding open and clogged pipe outlets on the streambank face. When pipeflow occurred, flow and sediment samples were collected using flow collection pans to quantify sediment concentrations. Flow and sediment data were used with an existing turbulent pipeflow and internal erosion model to estimate erodibility and critical shear stress properties of the soils, which were subsequently compared to similar properties derived from jet erosion tests. Clogged soil pipes resulted in pore water pressure increases in the soil adjacent to the pipe, which generally remained below saturation during these experimental periods, except at locations close to the plug. Depending on the density of the plugged soil material, the clogged soil pipes either burst, resulting in turbulent pipeflow, or were manually punctured to establish pipeflow. Calibrated critical shear stress from the turbulent pipeflow and internal erosion model matched that observed from jet erosion tests for the less erodible soils on the Dry Creek streambank, where sediment concentrations were consistently below 2 g L^{-1} even with fairly large hydraulic gradients on the pipe (0.3 m m^{-1}). Calibrated erodibility coefficients were much smaller than those measured with jet erosion tests. For the more erodible streambank soils of Cow Creek, sediment concentrations approached 40 g L^{-1} . There is a need for improved pipeflow modeling that accounts for rapidly changing pipe geometries, partially filled soil pipes, and pipeflow/soil matrix interactions.

Keywords. Erodibility, Internal erosion, Shear stress, Soil pipe, Streambank.

Streambank failure can be a significant contributor to sediment loads (Simon and Darby, 1999). Fluvial erosion is typically considered the main cause, while subsurface flow has been historically attributed to weakening streambanks as a result of increased soil water pressures reducing the soil strength (Rinaldi et al., 2008). Seepage, specifically the undercutting of banks by seepage erosion, has also been identified as a major contributor

(Hagerty, 1991; Fox et al., 2006a, 2007a; Wilson et al., 2007; Chu-Agor et al., 2008). In a review on subsurface flow contributions to hillslope and streambank instability, Fox and Wilson (2010) also noted the role of preferential flow through soil pipes. Pipeflow is an extreme form of preferential flow in which rapid flow occurs through a discrete flow path. There is no agreement as to what constitutes a soil pipe (Wilson et al., 2013), but Jones (2010) considered a soil macropore that exhibited a “water-sculptured form” to qualify as a soil pipe. Thus, the macropore must show evidence of internal erosion of the flow path. Internal erosion as a result of pipeflow has been credited for cataclysmic erosion events, such as levee and dam failures, landslides and debris flows, ephemeral and classic gully erosion, and streambank failures.

The pipeflow, particle detachment, and sediment transport processes involved are very complex. Internal erosion of a soil pipe is typically described by the classic excess shear stress equation:

$$q_s = k_{er} (\tau - \tau_c)^b \quad (1)$$

where q_s is the sediment transport rate ($\text{kg m}^{-2} \text{ s}^{-1}$), k_{er} is the erodibility coefficient (s m^{-1}), τ is the hydraulic shear stress on soil particles, and τ_c is the critical shear stress (Pa). This

Submitted for review in May 2012 as manuscript number SW 9755; approved for publication by the Soil & Water Division of ASABE in January 2013. Presented at the 2011 Symposium on Erosion and Landscape Evolution (ISELE) as Paper No. 11004.

The authors are **Taber L. Midgley, ASABE Member**, former NSF Graduate Research Fellow, Department of Biosystems and Agricultural Engineering, Oklahoma State University, Stillwater, Oklahoma; currently Project Engineer, AquaTera, Inc., Oklahoma City, Oklahoma; **Garey A. Fox, ASABE Member**, Associate Professor and Orville L. and Helen L. Buchanan Chair, Department of Biosystems and Agricultural Engineering, Oklahoma State University, Stillwater, Oklahoma; **Glenn V. Wilson, ASABE Member**, Hydrologist and Soil Physicist, USDA-ARS National Sedimentation Laboratory, Oxford, Mississippi; **Rachel Felice**, Graduate Research Assistant, Department of Biosystems and Agricultural Engineering, Oklahoma State University, Stillwater, Oklahoma; and **Derek Heeren, ASABE Member**, Assistant Professor, Department of Biological System Engineering, University of Nebraska, Lincoln, Nebraska. **Corresponding author:** Garey A. Fox, Department of Biosystems and Agricultural Engineering, 120 Ag Hall, Oklahoma State University, Stillwater, OK 74078; phone: 405-744-8423; e-mail: garey.fox@okstate.edu.

equation was developed for and typically applied to overland flow, which involves a two-dimensional planar surface. For a water-filled soil pipe, these forces act on the two-dimensional radial surface of the pipe and along its length, thereby enlarging the pipe circumference as a function of length along the soil pipe. For conditions in which a soil pipe extends through a reservoir's embankment, the relatively "infinite" supply of water from the imposed head of the reservoir can maintain water-filled conditions as the pipe enlarges (Bonelli et al., 2006). Flow rates increase as the pipe enlarges, thereby providing a positive feedback mechanism that results in more rapid internal erosion. Soil pipe enlargement progresses rapidly to the point at which the soil above can no longer be supported, and the soil pipe collapses, resulting in an embankment breach.

It has been postulated that such internal erosion can occur on hillslopes in which fully mature gullies can suddenly appear due to tunnel collapse (Swanson et al., 1989; Faulkner, 2006). However, for hillslope conditions in which such an "infinite" water supply is not available, the flow rate cannot continuously increase as the soil pipe enlarges. One result of the flow rate limitation is that soil pipes are only partially water-filled, and thus internal erosion enlarges the soil pipe at the pipe base. In laboratory experiments using a steady-state inflow rate applied to soil pipes, Wilson (2009) noted that the pipes tended to elongate at the base due to the pipes not being water-filled. These findings were also reported from field observations of erosion at the pipe base and not along the entire pipe circumference (Jones, 2010). The lack of shear stress on the pipe roofs, therefore, did not produce pipe collapse. When similar experiments were conducted using a constant head on the soil pipe (Wilson, 2011), pipe collapse was observed similar to pipe collapse features observed in the field (Zhang and Wilson, 2012). The similarities of these field observations with laboratory experiments suggest that, under some soil hydrologic conditions, hydraulic heads from either perched water tables or convergent flows into soil pipes can sufficiently maintain water-filled conditions to produce pipe collapse, at least under some limited linear distance of the soil pipe's length (Anderson et al., 2009).

The other result of flow rate limitations is that sediment transport can be transport limited instead of supply limited. Because the flow is not sufficient to transport all the internally eroded material out of the soil pipe, temporary clogging of the pipe can occur. It has been postulated that this clogging causes pressure buildups within soil pipes that can trigger landslides and debris flows (Pierson, 1983; Uchida et al., 2001; Kosugi et al., 2004); however, field measurements of this phenomenon are lacking. It is difficult enough to identify soil pipes *in situ*; to instrument a pressure sensor within a soil pipe and obtain data under such extreme cataclysmic conditions is almost prohibitive. As a result, laboratory experiments have been conducted to simulate conditions that can cause pressure buildups within soil pipes (see review by Wilson et al., 2013). Laboratory experiments using artificial pipes (e.g., Hele-Shaw chambers, PVC pipes, and acrylic pipes) have provided proof of principle that pressures could develop within pipes, but no measurements were made within these artificial pipes

(Pierson, 1983; Sidle et al., 1995; Kosugi et al., 2004). Sidle et al. (1995) simulated clogging by using pipe sections of increased internal roughness, which were created by impregnating the inside of PVC pipe with glass beads. Kosugi et al. (2004) simulated clogging by using closed-ended acrylic pipes, i.e., pipes that did not extend to the open bank face. Because these studies did not involve soil pipes, clogging from internally eroded material was prohibited. Wilson (2009, 2011) used soil pipes (i.e., voids created in soil by removing a rod from the soil) to study pipeflow and internal erosion. Tensiometers adjacent to the soil pipes showed minor pressure buildups, but pressures within the soil pipes were not measured. These studies documented the effect of sediment transport limitations by observing surges in flow associated with temporary clogging of soil pipes by internal erosion. Wilson et al. (2013) referred to such rapid internal erosion that caused soil pipes to clog as "mass failures of aggregated material." As a result, pipeflow was turbulent under both steady-state inflow and constant head.

In order to model turbulent pipeflow and internal erosion, previous research has used a deterministic solution developed by Bonelli et al. (2006). This solution uses two mass conservation equations, one for the water-particle mixture and one for the sediment particles, with interface erosion. The soil is assumed homogeneous and rigid, and hydraulic transfer between the matrix and pipe domains is neglected. The model assumes axisymmetrical flow with a large Reynolds number and uniform pressure across a section. Bonelli et al. (2006) assumed a linear relationship ($b = 1$) in the excess shear stress equation (eq. 1). The radius was assumed axially uniform, and the concentration was uniform in a section. As erosion occurs, a mass flux crosses the time-dependent interface; therefore, the interface between the fluid stream and the porous matrix undergoes a transition from solid-like to fluid-like behavior (Bonelli et al., 2006). The proposed model was shown to conform to experimental data from hole erosion tests (HET) on nine different soils.

Wilson et al. (2013) reviewed the experimental and numerical work conducted on pipeflow and resulting internal erosion. They identified the following knowledge gaps, which are relevant to this study: (1) "future work needs to be conducted under field conditions for a variety of soils and hydrologic conditions. Such research could include created or natural soil pipes but should also provide observations of soil water pressures within the soil pipes and in the soil immediately adjacent to the soil pipe at locations where clogging occurs"; and (2) with regard to modeling pipeflow and internal erosion, "advances are needed in the ability to model the preferential flow, sediment detachment, internal mass failures, and sediment transport processes associated with internal erosion of soil pipes." No study to date has made *in situ* measurements of pipeflow and internal erosion associated with streambanks or the pressure buildups associated with pipe clogging. Studies have simply reported the presence and number of macropores or soil pipes on streambanks (e.g., Fox et al., 2007a). Given the limited field work conducted to date on quantifying and modeling these processes, the objectives of this study were

to (1) investigate pore water pressure dynamics around open and clogged soil pipes under field conditions; (2) compare pipeflow, internal erosion, and pipe enlargement for soil pipes created in two contrasting soil types; (3) investigate the use of existing pipeflow models based on excess shear stress formulations for streambank piping; and (4) determine if jet erosion tests (JETs) could provide reasonable estimates of excess shear stress parameters for soil piping.

MATERIALS AND METHODOLOGY

FIELD EXPERIMENTS: SITE SELECTION AND SETUP

Two locations were selected to conduct field experiments under controlled conditions. Dry Creek (33.7485° N, 89.1725° W), located in Chickasaw County, Mississippi, is a tributary to Little Topashaw Creek (LTC), a 37 km² experimental subwatershed of the Topashaw Canal CEAP watershed in Mississippi (Wilson et al., 2008). The creek flows through alluvial plains under cultivation that are surrounded by forested areas. Wilson et al. (2008) identified excess sediment as the main water quality issue within this watershed. Dry Creek is a deeply incised stream with nearly 90° banks consisting of Urbo silty clay loam soils (fine, mixed active, acid, thermic Vertic Epiaquepts) (Rhoades et al., 2007). Midgley et al. (2012) reported that the site has a clay loam (37% sand, 34% silt, and 29% clay) surface soil with a bulk density near 1.6 g cm⁻³. Site setup at Dry Creek

included the installation of an injection trench and a tensiometer network to observe soil pore water pressures (fig. 1a). The injection trench was a frame structure inserted beneath the ground in which a constant head could be maintained. The structure contained a perforated side facing the streambank to allow easy water passage. Gravel was added between the structure and the surrounding soil. The trench was located 2.8 m from the bank face. The location of the trench was decided based on maintaining a safe distance from the edge of the creek for installing the trench with a backhoe and Giddings drill rig. The trench was utilized for an earlier seepage erosion and undercutting study (Midgley et al., 2012).

Located in Payne County, Oklahoma (36.1213° N, 97.0998° W), Cow Creek is currently deepening and widening with the formation of associated side gullies (Lovern and Fox, 2012). Streambanks consist of a Pulaski fine sandy loam (coarse-loamy, mixed, superactive, nonacid, thermic Udic Ustifluvents) with a sandy loam surface (72% sand, 13% silt, and 15% clay). The setup on Cow Creek included the installation of an injection trench similar to the installation on Dry Creek as described above, approximately 4 m from the bank face (fig. 1b). The trench was installed at this location for an earlier study investigating seepage mechanisms of bank instability, and again the location was determined based on a safe distance for installation.

Two types of experiments were conducted (table 1): open pipe experiments, which involved soil pipes that were open the entire length from the trench to the bank face, and

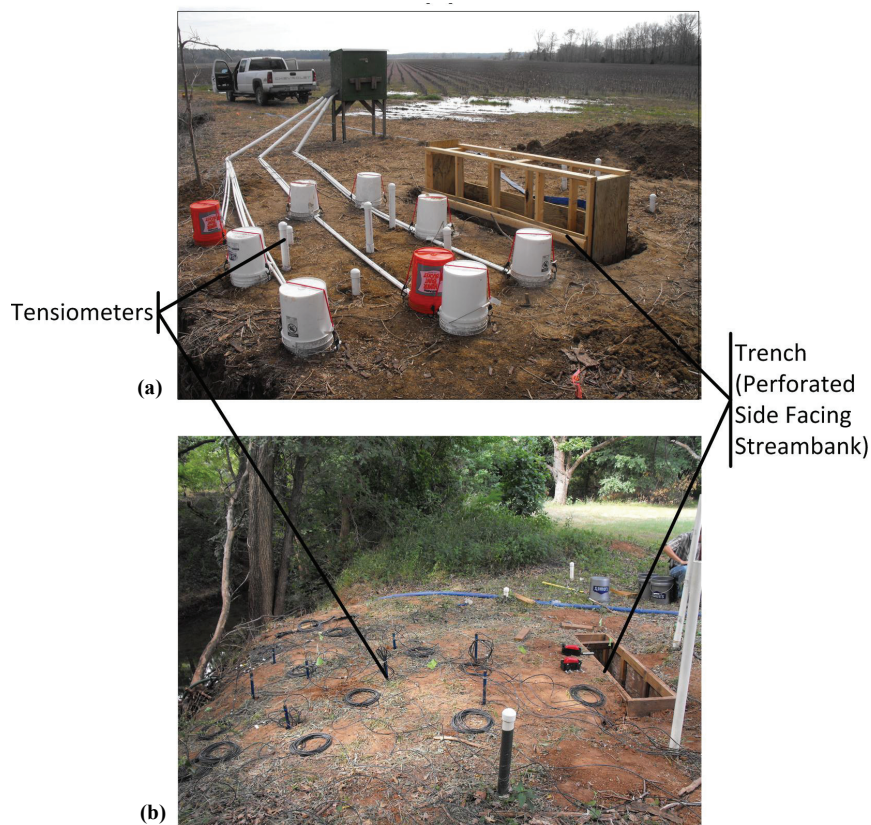


Figure 1. Trench installed adjacent to (a) Dry Creek and (b) Cow Creek streambanks. Tensiometer networks were installed for monitoring pore water pressures. The side of the trench closest to the streambank was perforated to allow flow into the soil pipe.

clogged pipe experiments, which involved plugging the outlet of the soil pipe using soil excavated adjacent to the pipe. The experiments involved applying a constant head to the soil pipe at the opening to the trench (open pipe) and measuring flow and sediment concentrations during pipe-flow as well as soil water pressures adjacent to the soil pipe. Soil pipes were created by driving a rod from the bank face back to the trench (fig. 2). A series of rods (1.82 m long, 0.95 cm dia.) with connectors (7.6 cm long, 2.9 cm dia.) and tips were driven into the bank by hammering until the tip reached the trench. A smaller rod (0.9 m long) was connected to previously inserted rods for hammering at the streambank face. When the connected rods reached the trench, they were driven through the gravel surrounding the trench and the wood frame to expose the opening of the soil pipe. The rods were then removed from the bank face through the created soil pipe. Soil pipes had slopes less than 2.5% after manual installation of the rods at both field sites. The pipe size and water pressure heads were determined based on previous experimental studies in the laboratory (Wilson et al., 2013) and field observations of macropores at bank faces (Fox et al., 2007a).

The clogged pipe experiments involved establishing a constant head on the trench and measuring soil water pressures until the clog in the soil pipe was removed or the test was terminated. For clogged pipe experiments, soil was packed into the last 15 to 30 cm of the soil pipe at a specified bulk density. When the pipe was packed to create the clogged pipes, similar diameter, triplicate PVC pipes were also packed at approximately the same compaction effort to determine the bulk density of the clog. T5 tensiometers (UMS GmbH, Munich, Germany; 10 or 15 cm shaft lengths) were installed in the bank face near the pipe exit to monitor pore water pressures in this area. These tensiometers were installed in the manner shown in figure 3 for Dry Creek (14.5 cm insertion depth) and figure 4 for Cow Creek (9.5 cm insertion depth). Note that at Cow Creek the soil pipe had enlarged from previous open pipe experiments to the extent that the tensiometers were installed directly into the clogged section of the soil pipe.

When pipeflow occurred, flow and sediment samples were collected using flow collection pans installed into the bank face beneath soil pipe outlets. The pans routed flow to a PVC pipe, which led down the streambank where samples were collected. Containers (18.9 L) were used to collect the flow and sediment. Each container's mass was measured,



Figure 2. Rod being driven into soil of Dry Creek (top) and Cow Creek (bottom) to create a soil pipe that extends from bank to trench.

and then a sediment sample was acquired after manually agitating the bucket's contents to evenly distribute the sediment.

Along with the pipeflow experiments, jet erosion tests (JETs; Hanson, 1990) were conducted on the bank face at the depths of the soil pipes at each site for quantifying the JET k_{er} and τ_c of the soils. In order to create a measurable scour hole from which k_{er} and τ_c can be calculated, the jet test device directs a jet of water toward the soil. For this research, a pump was used to provide water to an adjustable constant-head reservoir, which powered the jet. The head for the jet was set near a level that the streambank would

Table 1. Experimental conditions for the soil pipe experiments at the two streambank sites.

Site	Type of Pipe (and bulk density of plug)	Water Head	Measurements
Dry Creek	Clogged and then open (0.8 g cm ⁻³ for 30 cm)	15 cm for 15 min	Flow, sediment, and pore water pressure (plug failed immediately)
	Clogged (1.1 g cm ⁻³ for 30 cm)	15 cm for 60 min and 30 cm for 187 min	Pore water pressure (plug remained intact)
	Clogged and then open (1.1 g cm ⁻³ for 30 cm)	48 cm for 188 min and 92 cm for 190 min	Flow, sediment, and pore water pressure (plug was punctured manually after 278 min)
Cow Creek	Open	15 cm for 15 min and 30 cm for 15 min	Pore water pressure (pipe clogged internally)
	Open	30 cm for 45 min	Flow, sediment, and pore water pressure
	Clogged and then open (1.3 g cm ⁻³ for 15 cm)	30 cm for 4 min	Pore water pressure (flow began at 2 min; plug failed completely after 3 min)

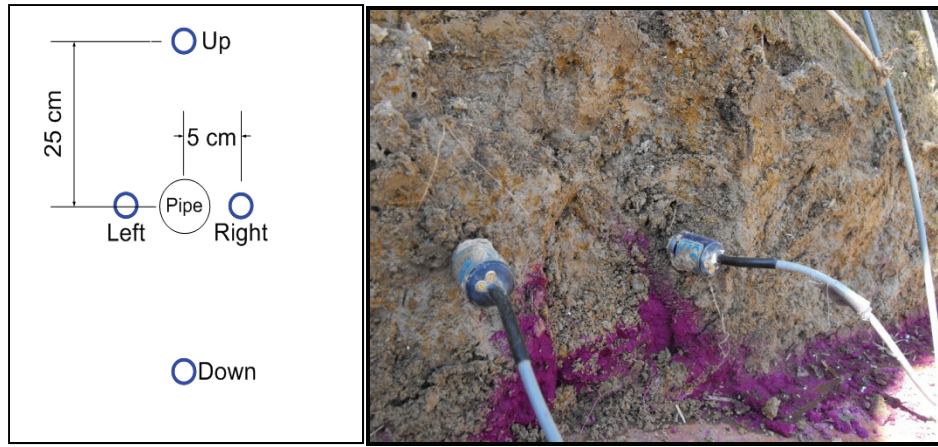


Figure 3. Diagram of T5 tensiometer installation near exit of soil pipe for Dry Creek (left) and photo of clogged pipe and adjacent tensiometers (right). Tensiometers had a 15 cm shaft length. Red dye stains were Rhodamine WT that was included as a tracer in the injected water.

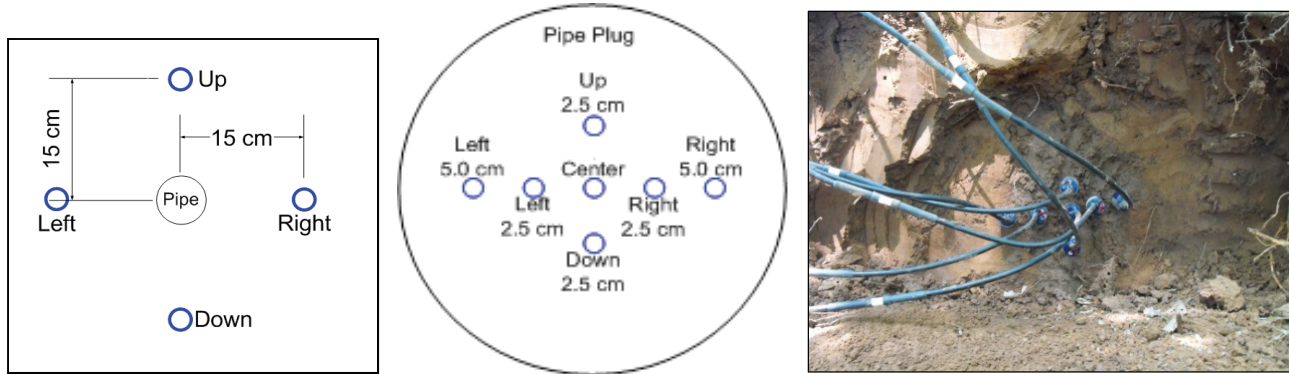


Figure 4. Diagram of T5 tensiometer installation near exit of pipes for Cow Creek for open pipe experiments (left) and clogged pipe experiments (center), and photo of tensiometers for clogged pipe experiments (right). Tensiometers had a 10 cm shaft length.

have experienced during a flood event. A base for the jet test device was driven into the soil at the desired test location. The soil and the steel ring of the base acted as the bottom of the submergence tank. The device was then placed on the base and locked in, sealing the device to the base. The submergence tank was filled with water, and testing was initiated. Periodically, the jet was blocked with a deflector plate, and an installed point gauge was then used to measure the depth of the scour hole. Measurements were taken until the scour depth reached an equilibrium depth. Four *in situ* JETs were conducted on both the Cow Creek and Dry Creek streambanks.

MODELING

The flow rate and sediment concentration data from each experiment were used to evaluate the Bonelli et al. (2006) pipeflow model. Based on a soil pipe of length L and initial radius R_o , the model predicted the radius of the pipe, $R(t)$, as a function of time (t), mean longitudinal velocity, $V(t)$, and the corresponding flow rate, $Q(t)$:

$$\frac{R(t)}{R_o} = 1 + \left(1 - \frac{\tau_c}{P_{fl}}\right) \left[\exp\left(\frac{t}{t_{er}}\right) - 1\right] \quad (2a)$$

$$\frac{V(t)}{V_{fl}} = \sqrt{\frac{R(t)}{R_o}} \quad (2b)$$

$$Q(t) = Q_{fl} \left(\frac{R(t)}{R_o}\right)^{5/2} \quad (2c)$$

where t_{er} is a characteristic erosion time (s), which depends on k_{er} , L , and the density of the sediment (ρ_g), as shown in equation 3; P_{fl} is the assumed constant hydraulic stress (Pa) as a function of the input (p_{in}) and output pressures (p_{out}), as shown in equation 4; Q_{fl} is the initial entrance flow ($m^3 s^{-1}$); and V_{fl} is a reference velocity ($m s^{-1}$), as shown in equation 5:

$$t_{er} = \frac{2L\rho_g}{k_{er}(p_{in} - p_{out})} \quad (3)$$

$$P_{fl} = \frac{R_o(p_{in} - p_{out})}{2L} \quad (4)$$

$$V_{fl} = \frac{Q_{fl}}{\pi R_o^2} \quad (5)$$

From these equations, it is possible to derive an equation for the shear stress at the interface (τ):

$$\tau = P_{fl} \frac{R(t)}{R_o} \quad (6)$$

This research also derived sediment concentration equations not originally reported by Bonelli et al. (2006). Using equations 1 and 6, the erosion rate (q_s) can then be combined with the predicted $Q(t)$ to estimate the eroded concentration, $C(t)$:

$$C(t) = \frac{q_s(t)A}{Q(t)} = \frac{2\pi R(t)Lq_s(t)}{Q(t)} \quad (7)$$

An alternative but equivalent form can be derived from the predicted $R(t)$ during a specified time interval (Δt):

$$C(t) = \frac{\pi(R(t)^2 - R_o^2)L\rho_g}{Q(t)\Delta t} \quad (8)$$

The flow rates and sediment concentration data from each of the experiments were modeled by fitting k_{er} and τ_c based on minimizing the sum of squared errors between observed and predicted flow rates and sediment concentrations during the experimental period. The quality of the model fit was assessed based on the root mean square error and a normalized objective function (Fox et al., 2006b, 2007b):

$$RMSE = \sqrt{\frac{\sum_{i=1}^n (X_i - Y_i)^2}{n}} \quad (9)$$

$$NOF = \frac{RMSE}{X_a} \quad (10)$$

where X_i and Y_i are the observed and predicted flow rates or sediment concentrations, respectively; X_a is the mean of observed values; and n is the number of observations. In general, 1%, 10%, and 50% deviations from the observed values result in NOF values of 0.01, 0.10, and 0.50, respectively.

RESULTS AND DISCUSSION

JET EROSION TESTS

JETs demonstrated the difference in k_{er} and τ_c of the two

streambanks. As expected, the sandy loam soil of Cow Creek was a much more erodible soil, with $k_{er} = 1.0 \times 10^{-1} \text{ s m}^{-1}$ (standard deviation of $7.1 \times 10^{-2} \text{ s m}^{-1}$) and $\tau_c < 0.1 \text{ Pa}$ (measured consistently among all four tests). The clay loam soil of Dry Creek was less erodible: $k_{er} = 2.8 \times 10^{-2} \text{ s m}^{-1}$ (standard deviation of $2.7 \times 10^{-2} \text{ s m}^{-1}$) and $\tau_c = 7.9 \text{ Pa}$ (standard deviation of 9.3 Pa).

DRY CREEK CLOGGED PIPE EXPERIMENT: LOW-DENSITY PLUG

In this experiment, the last 30 cm of the pipe was clogged using a loose plug of approximately 0.8 g cm^{-3} density, mimicking sloughed material that may have blocked the exit of the pipe. The plug was flushed out of the pipe almost immediately, and pipeflow was initiated upon application of the head in the trench. A 15 cm head was maintained for 15 min in the trench. The tensiometers installed in the bank face did not show a response. Figure 5 shows the recorded flow rate data and the Bonelli et al. (2006) model calibrated to match the data ($Q_{fl} = 13 \text{ L min}^{-1}$, $R_o = 2.9 \text{ cm}$, $L = 2.8 \text{ m}$, $k_{er} = 5 \times 10^{-4} \text{ s m}^{-1}$, and $\tau_c = 4.9 \text{ Pa}$). Note that the model was only calibrated to flow and sediment concentration data at times greater than 3 min into the experiment. The reason was that flow rate data initially increased due to the reopening of the pipe (clog removal) and then leveled off approximately 3 min after flow initiated as the pipe at the bank face reached the original diameter.

Sediment concentrations are also shown in figure 5. The data values were initially higher due to the erosion of the pipe clog at the beginning of the experiment. After removal of the clog, the erosion of the pipe walls was limited, meaning that the pipe radius and therefore flow area could not expand, resulting in fairly constant flow rates and sediment concentrations. The pipe exit only slightly enlarged beyond the diameter at which it was created. The estimated k_{er} from the calibration was much smaller than the k_{er} reported from JETs, possibly due to the high-density pipe “skin” (i.e., consolidated soil on the pipe walls) created during installation of the soil pipe in contrast to the intact soil for the JETs, but the τ_c matched.

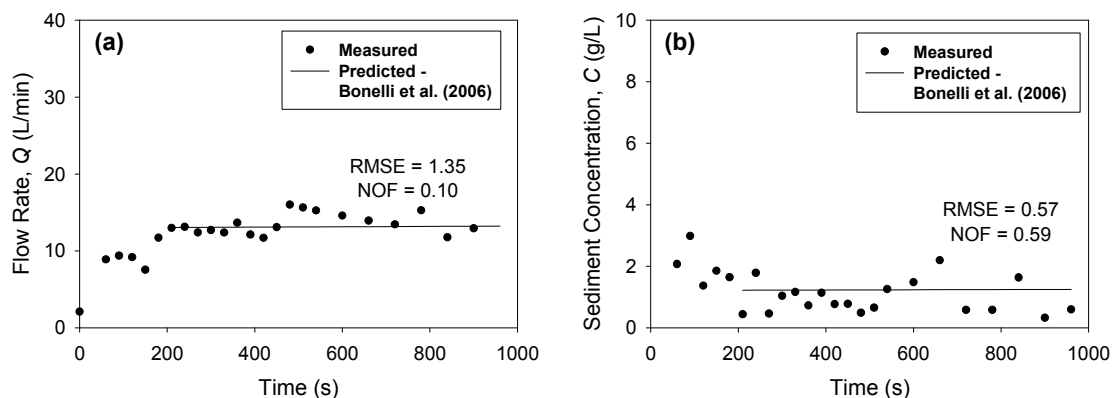


Figure 5. Observed (a) flow and (b) sediment concentrations for the low-density plug experiment at Dry Creek and Bonelli et al. (2006) model fit to both flow rates and sediment concentration (RMSE = root mean square error and NOF = normalized objective function).

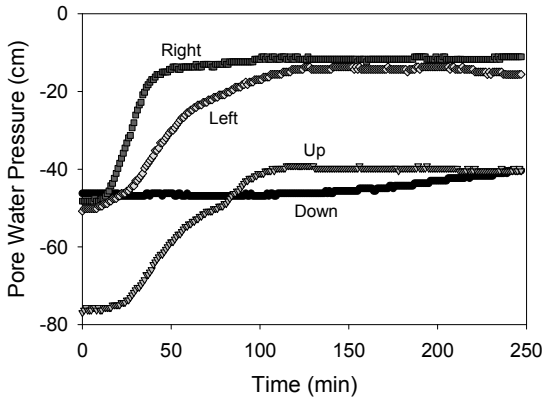


Figure 6. Pore water pressures of tensiometers installed 25 cm above and below the pipe exit (up and down) and 5 cm to the left and right of the pipe exit (left and right) for the first high-density plug experiment (clogged pipe) at Dry Creek.

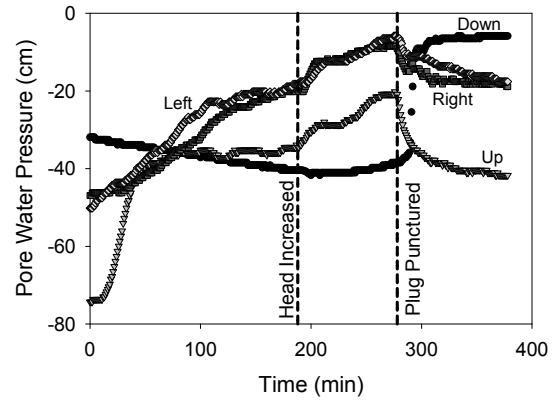


Figure 7. Pore water pressures observed from tensiometers installed 25 cm above and below the pipe (up and down) and 5 cm to the right and left of the pipe (left and right) for the second high-density plug experiment (clogged pipe) at Dry Creek.

**DRY CREEK CLOGGED PIPE EXPERIMENTS:
HIGH-DENSITY PLUG**

Two clogged-pipe experiments were conducted using tighter plugs at a density of 1.1 g cm^{-3} over the final 30 cm at the exit of the pipe. In the first experiment, a 15 cm head above the inlet of the pipe was applied for 60 min in the trench, after which the head was increased to 30 cm for an additional 187 min. The plug never failed, so there was no flow. The tensiometers near the plug approached steady state but never reached saturation, as indicated in figure 6.

This experiment was repeated using the same plug density (1.1 g cm^{-3}) and length (30 cm). Head was maintained at 48 cm for the first 188 min of the experiment. The plug did not fail, and again the tensiometers responded with increased pore water pressures in the soil near the clog (fig. 7). The constant head was then increased to 92 cm for an additional 90 min, and still the plug did not fail. Finally, after 278 min, the plug was manually punctured with a 1 mm rod, and flow was established through the newly opened soil pipe. Flow rates and sediment concentrations were recorded for the next 100 min. Tensiometer responses near the exit of the pipe suggested slowly increasing soil water pressures while the clog was in place and rapid decreases in pressures around the soil pipe when the clog was punctured, except for the tensiometer that was below the pipe exit (fig. 7).

Flow rate data and the fitted Bonelli et al. (2006) model ($Q_{fl} = 30 \text{ L min}^{-1}$, $R_o = 2.9 \text{ cm}$, $L = 2.8 \text{ m}$, $k_{er} = 7 \times 10^{-6} \text{ s m}^{-1}$, and $\tau_c = 3.5 \text{ Pa}$) are shown in figure 8. Flow rates were only approximately twice as high as in the earlier Dry Creek experiment, even though the head was larger (92 cm compared to 15 cm) in this experiment, most likely due to the initial size (1 mm) of the opening at the pipe clog. Similar to the previous experiment, the early-time data demonstrated rapidly increasing flow rates over time due to the increase in the flow area as the opening expanded in the punctured pipe clog. Approximately 30 min into the experiment, flow rates and sediment concentrations stabilized, demonstrating fairly non-erodible material even at these high imposed heads, and therefore the model was applied only to these late-time data. Sediment concentrations are also shown in figure 8 and again were fairly constant based on the observed data. Even with these higher shear stresses due to the higher head, the material was resistant to erosion and the pipe was unable to measurably expand. The τ_c derived from the calibrated model was within the range of measurements reported from JETs with smaller calibrated k_{er} .

COW CREEK OPEN PIPE EXPERIMENTS

Two open pipe experiments were performed at Cow Creek. In the first experiment, a 15 cm head was applied on

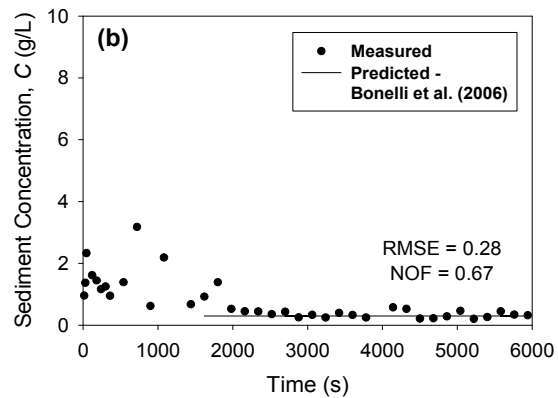
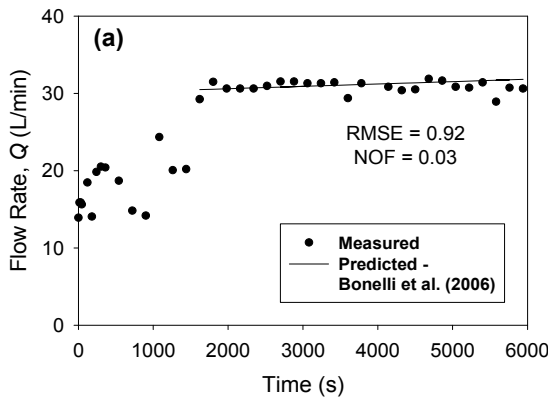


Figure 8. Observed (a) flow and (b) sediment concentrations for the second high-density plug experiment (clogged pipe) at Dry Creek and Bonelli et al. (2006) model fit to both flow rates and sediment concentrations. Time was initiated when the plug was punctured in the experiment (RMSE = root mean square error and NOF = normalized objective function).

the soil pipe inlet in the trench. Three minutes after flow initiation from the exit of the pipe, flow slowed and stopped. Head was maintained at 15 cm for 15 min and then increased to 30 cm for an additional 15 min. Flow never started, and there was no tensiometer response. Internal erosion of the sandy loam material inside the pipe caused a pipe collapse and clogging. Subsequent reopening of the pipe revealed that the clogging occurred near the pipe inlet at the trench.

The second experiment applied a 30 cm head for 45 min to the reopened soil pipe. Flow never stopped during the experiment. Flow rates and sediment concentrations for this open pipe experiment are shown in figure 9. Flow rates initially increased slowly and then increased rapidly approximately 16 to 17 min into the experiment. Since the pipe was initially empty, the pipe most likely was not flowing full along its entire length during the early stages of the experiment as the head built up over the 4 m pipe length. It is likely that the pipe was not full during later stages as well due to the rapid expansion at the base of the pipe by internal erosion and the hydraulic losses into a network of naturally occurring soil macropores and other pipes. The conductivity of this soil may have created significant exchange between the pipe and soil matrix during the early part of the experiment, such that the pipe may have been eroding in the upper reaches of the soil pipe while flow was transferred from the soil pipe into the soil matrix further along the pipe. In addition, the presence of roots in the bank likely provided a network of preferential flow paths through which water could be lost to the soil pipe and elude the measurement devices. Flow rates into the soil pipe may have been increasing, but no measureable difference in flow out of the soil pipe was observed due to transfer into the soil matrix and other macropores or soil pipes. Correspondingly, sediment concentrations relative to the flow exiting the pipe were increasing during the first 16 to 17 min but then approached an asymptote and even declined as the experiment continued.

Unlike the less erodible and less conductive Dry Creek soil, the model was unable to fit both data sets (flow rates and sediment concentrations) simultaneously for this soil because of the inherent assumptions associated with the Bonelli et al. (2006) model (i.e., full pipeflow and no inter-

action between matrix and soil pipe domains). These results suggest the need for improved pipeflow models that better account for pipeflow and soil matrix interactions. Fitting just the flow rate data with late-time data when interaction between the soil matrix and pipe domains would be hypothesized as being less pronounced (fig. 9), the Bonelli et al. (2006) model suggested the following parameters: $Q_{fl} = 9 \text{ L min}^{-1}$, $R_o = 2.9 \text{ cm}$, $L = 4.0 \text{ m}$, $k_{er} = 0.1 \text{ s m}^{-1}$, and $\tau_c = 0 \text{ Pa}$, suggesting a much more erodible soil at Cow Creek than at Dry Creek. Note the consistency between the k_{er} and τ_c measured with the JETs and calibrated from the Bonelli et al. (2006) model.

COW CREEK CLOGGED PIPE EXPERIMENT

This was a clogged pipe experiment in which a clean vertical face was dug around the exit of the previously eroded pipe and then plugged with excavated soil at 1.3 g cm^{-3} over the last 15 cm of the pipe. Tensiometers were installed in the arrangement shown in figure 4 (center), and the tensiometer responses are shown in figure 10. One minute into the experiment, flow was exiting the bank face through macropores near the soil pipe. Flow began seeping through the plug at around 2 min, and the plug failed completely after 3 min. This supports the hypothesis that substantial water transfer was occurring between the soil pipe and the adjacent soil matrix and preferential flow paths. The tensiometer in the center of the arrangement (fig. 4) was positioned within the soil pipe plug. This tensiometer showed a dramatic pressure buildup, quickly exhibiting positive values, in response to flow initiation through the plug. Note that the tensiometers positioned 2.5 cm away from the pipe center generally showed a fast pressure buildup to positive pressures (fig. 10). The 2.5 cm tensiometers were positioned within the soil pipe plug at the beginning of the experiment. The 5.0 cm tensiometers, positioned within the soil matrix adjacent to the plug, exhibited either no response or a slow response. The tensiometer located 5.0 cm to the left of the plug started at 0 cm pore water pressure; this was most likely due to tensiometer error, potentially the result of poor contact with the soil. In general, there was a significant hydraulic non-equilibrium with a high gradient into the soil matrix. This is the first study to document pressure buildups within a soil pipe clog under

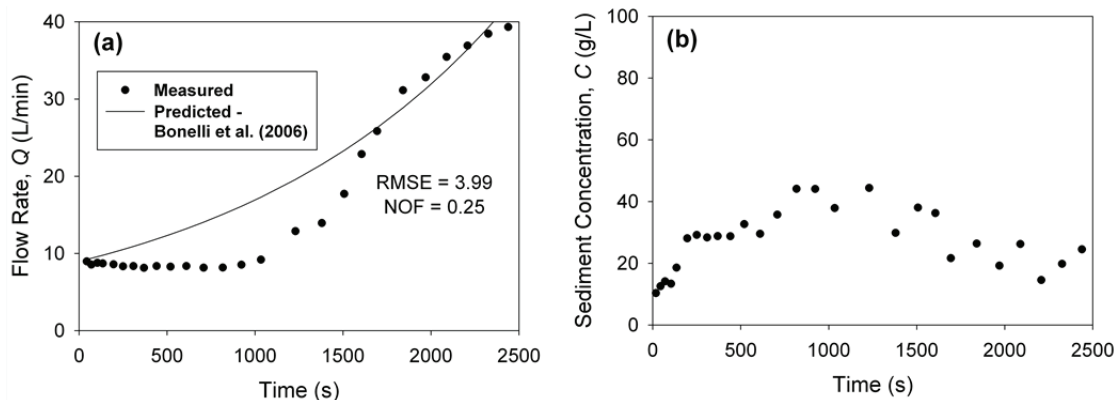


Figure 9. Observed (a) flow rates and (b) sediment concentrations for the open soil pipe experiment at Cow Creek and Bonelli et al. (2006) model fit to the flow rate data. The model was unable to simultaneously fit both the flow rate and sediment concentration data.

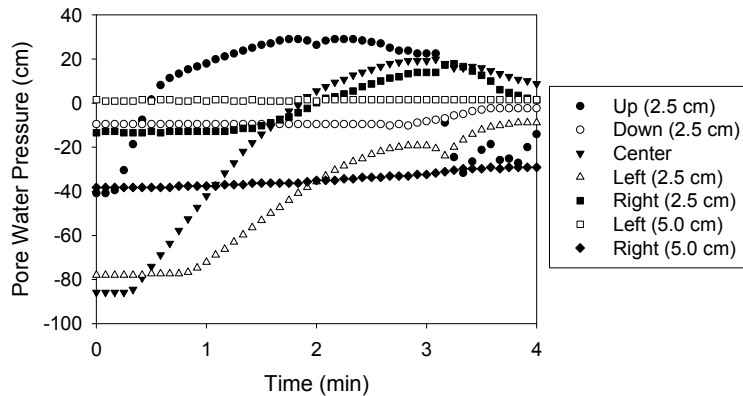


Figure 10. Tensiometer response for the clogged pipe experiment on Cow Creek. Tensiometer locations refer to the center diagram in figure 4.

field conditions, thereby confirming the proposed mechanism of landslide failure (Uchida et al., 2001).

SUMMARY AND CONCLUSIONS

Clogged soil pipes resulted in pore water pressure increases in the adjacent soil and within the clogged soil pipe, which could result in destabilization of the surrounding soil material and lead to bank failure. Pore water pressure increases were typically greatest within the soil pipe clog, but pressure increases were observed in the adjacent soil as much as 25 cm away from the soil pipe. The clogged soil pipes either burst when plugged with a low-density soil material (less than 1.0 g cm^{-3} , which might simulate sloughed material from previous bank failures) or were resistant to removal by the pore water pressure gradients established during the experimental conditions in this research for these soil types. It is hypothesized that additional time for saturation and establishment of hydraulic gradients in the plug material would eventually lead to opening of the soil pipe and turbulent pipeflow. Preferential flow around resistant clogs and manually reopening resistant clogs suggest that such clogging, with time, would eventually reopen the clogged pipe or create an alternate new pipe. More research needs to be performed on enlargement and clogging of soil pipes by internal erosion, pore water pressures within the open portion of the pipe during clogging, and mass failure processes.

Calibrated τ_c from the turbulent pipeflow and internal erosion model matched that observed from jet erosion tests for the less erodible soils on the Dry Creek streambank, but the model tended to predict much smaller k_{er} than measured with the jet erosion tests. Even when imposing hydraulic gradients of 0.05 to 0.3 m m^{-1} , the resulting sediment concentrations in the 15 to 30 L min^{-1} flow were consistently less than 2 g L^{-1} . For the more erodible streambank soils of Cow Creek, inherent turbulent pipeflow and internal erosion model assumptions of full pipeflow and no interaction between the matrix and soil pipe domains do not appear to apply. Using a subset of the complete data, estimated erodibility coefficients and critical shear stresses from the jet erosion tests were similar to those estimated with the calibrated turbulent pipeflow and internal erosion model.

There is a need for improved pipeflow models that better

account for rapidly changing pipe geometries, pipe clogging, and pipeflow and soil matrix interactions, especially for erodible soils with a network of preferential flow paths. The assumption of an infinite water supply source for streambanks and other hillslopes is inadequate for most cases in terms of the upslope contribution of water to the soil pipe. Even a constant-head injection trench could not provide the necessary constant head to keep the soil pipe flowing full due to the rapid erosion of the soil pipe at the base in the more erodible soil and the presence of additional macropores and soil pipes in the root-permeated streambank. Additional research is also needed to better understand the internal erosion and pipe clogging process, as this appeared to be an important process in the more erodible soils investigated in this research.

ACKNOWLEDGEMENTS

The authors wish to thank the technical support personnel (Mick Ursic, Don Seale, Alan Hudspeth, Allen Gregory, and Brian Bell) at the USDA-ARS National Sedimentation Laboratory in Oxford, Mississippi, for their assistance with instrumentation and data collection for this project. This material is based on work supported by the National Science Foundation (NSF) under Grant No. 0943491 and an NSF Graduate Research Fellowship. Any opinions, findings, and conclusions or recommendations expressed in this material are those of the authors and do not necessarily reflect the views of the National Science Foundation.

REFERENCES

- Anderson, A. E., M. Weiler, Y. Alila, and R. O. Hudson. 2009. Dye staining and excavation of a lateral preferential flow network. *Hydrol. Earth Syst. Sci.* 13(6): 935-944.
- Bonelli, S., O. Brivois, R. Borghi, and N. Benahmed. 2006. On the modelling of piping erosion. *Comptes Rendu Mecanique* 334(8-9): 555-559.
- Chu-Agor, M. L., G. V. Wilson, and G. A. Fox. 2008. Numerical modeling of bank instability by seepage erosion undercutting of layered streambanks. *J. Hydrol. Eng.* 13(12): 1133-1145.
- Faulkner, H. 2006. Piping hazard on collapsible and dispersive soils in Europe. In *Soil Erosion in Europe*, 537-562. J. Boardman and J. Poesen, eds. Chichester, U.K.: John Wiley and Sons, Ltd.
- Fox, G. A., and G. V. Wilson. 2010. The role of subsurface flow in

- Fox, G. A., G. V. Wilson, R. K. Periketi, and B. F. Cullum. 2006a. Sediment transport model for seepage erosion of streambank sediment. *J. Hydrol. Eng.* 11(6): 603-611.
- Fox, G. A., G. J. Sabbagh, W. Chen, and M. Russell. 2006b. Uncalibrated modeling of conservative tracer and pesticide leaching to groundwater: Comparison of potential Tier II exposure assessment models. *Pest Mgmt. Sci.* 62(6): 537-550.
- Fox, G. A., G. V. Wilson, A. Simon, E. Langendoen, O. Akay, and J. W. Fuchs. 2007a. Measuring streambank erosion due to ground water seepage: Correlation to bank pore water pressure, precipitation, and stream stage. *Earth Surf. Proc. Land.* 32(10): 1558-1573.
- Fox, G. A., S. H. Pulijala, and G. J. Sabbagh. 2007b. Influence of rainfall distribution on simulations of atrazine, metolachlor, and isoxaflutole/metabolite transport in subsurface drained fields. *J. Agric. Food Chem.* 55(14): 5399-5407.
- Hagerty, D. J. 1991. Piping/sapping erosion: 1. Basic considerations. *J. Hydraul. Eng.* 117(8): 991-1008.
- Hanson, G. J. 1990. Surface erodibility of earthen channels at high stresses: II. Developing an *in situ* testing device. *Trans. ASAE* 33(1): 132-137.
- Jones, J. A. A. 2010. Soil piping and catchment response. *Hydrol. Proc.* 24(12): 1548-1566.
- Kosugi, K., T. Uchida, and T. Mizuyama. 2004. Numerical calculation of soil pipe flow and its effect on water dynamics in a slope. *Hydrol. Proc.* 18(4): 777-789.
- Lovern, S. B., and G. A. Fox. 2012. The streambank research facility at Oklahoma State University. *Resource* 19(2): SP10-SP11.
- Midgley, T. L., G. A. Fox, G. V. Wilson, D. M. Heeren, E. J. Langendoen, and A. Simon. 2012. Streambank erosion and instability induced by seepage: In-situ injection experiments. *J. Hydrol. Eng.* (in press): doi: 10.1061/(ASCE)HE.1943-5584.0000685.
- Pierson, T. C. 1983. Soil pipes and slope stability. *Qtly. J. Eng. Geol. and Hydrogeol.* 16(1): 1-11.
- Rhoades, P. R., L. Oldham, and G. V. Wilson. 2007. Data compilation for Conservation Effects Assessment Project: Yalobusha River watershed, Final report. Tech. Report No. 51. Oxford, Miss.: USDA-ARS National Sedimentation Laboratory.
- Rinaldi, M., B. Mengoni, L. Luppi, S. E. Darby, and E. Mosselman. 2008. Numerical simulation of hydrodynamics and bank erosion in a river bend. *Water Resour. Res.* 44: W09428, doi: 10.1029/2008WR007008.
- Sidle, R. C., H. Kitahara, T. Terajima, and Y. Nakai. 1995. Experimental studies on the effects of pipeflow on throughflow partitioning. *J. Hydrol.* 165(1-4): 207-219.
- Simon, A., and S. E. Darby. 1999. The nature and significance of incised river channels. In *Incised River Channels: Processes, Forms, Engineering, and Management*, 3-18. S. E. Darby and A. Simon, eds. New York, N.Y.: John Wiley and Sons.
- Swanson, M. L., G. M. Kondolf, and P. J. Boison. 1989. An example of rapid gully initiation and extension by subsurface erosion: Coastal San Mateo County, California. *Geomorphology* 2(4): 393-403.
- Uchida T., K. Kosugi, and T. Mizuyama. 2001. Effects of pipeflow on hydrological process and its relation to landslide: A review of pipeflow studies in forested headwater catchments. *Hydrol. Proc.* 15(11): 2151-2174.
- Wilson, G. V. 2009. Mechanisms of ephemeral gully erosion caused by constant flow through a continuous soil-pipe. *Earth Surf. Proc. Land.* 34(14): 1858-1866.
- Wilson, G. V. 2011. Understanding soil-pipeflow and its role in ephemeral gully erosion. *Hydrol. Proc.* 25(15): 2354-2364.
- Wilson, G. V., R. K. Periketi, G. A. Fox, S. M. Dabney, F. D. Shields Jr., and R. F. Cullum. 2007. Seepage erosion properties contributing to streambank failure. *Earth Surf. Proc. Land.* 32(3): 447-459.
- Wilson, C. G., R. A. Kuhnle, D. D. Bosch, J. L. Steiner, P. J. Starks, M. D. Tomer, and G. V. Wilson. 2008. Quantifying relative contributions from sediment sources in Conservation Effects Assessment Project watersheds. *J. Soil Water Conserv.* 63(6): 523-531.
- Wilson, G. V., J. Nieber, R. C. Sidle, and G. A. Fox. 2013. Internal erosion during soil pipeflow: State of the science for experimental and numerical analysis. *Trans. ASABE* 56(2): 465-478.
- Zhang, T., and G. V. Wilson. 2012. Spatial distribution of collapsed pipes in Goodwin Creek watershed, Mississippi. *Hydrol. Proc.* (in press): doi: 10.1002/hyp.9357.